

The Effect of Stator Inter-Turn Short-Circuit Fault on DFIG Performance Using FEM

Hacene Mellah

Department of Electrical Engineering
Akli Mohand Oulhadj University of Bouira
Bouira, Algeria
has.mel@gmail.com

Serdal Arslan

Organized Industrial Zone Vocational Higher School
Harran University
Sanliurfa, Turkey
elkserdal@gmail.com

Sahraoui Hamza

Department of Electrical Engineering
Benbouali Hassiba University of Chlef
Chlef, Algeria
hamzasahraoui@gmail.com

Kamel Eddine Hemsas

Department of Electrical Engineering
Ferhat Abbas Sétif 1 University
Sétif, Algeria
hemsas.kamel@gmail.com

Saoudi Kamel

Department of Electrical Engineering
Akli Mohand Oulhadj University of
Bouira, Bouira, Algeria
k.saoudi@univ-bouira.dz

Received: 24 March 2022 | Revised: 15 April 2022 | Accepted: 18 April 2022

Abstract-Doubly-Fed Induction Generators (DFIG) are operated for wind energy production, and as their capacity is increasing, their safety and reliability become more important. Several faults affect the performance of DFIG. The stator winding Inter-Turn Short-Circuit Fault (ITSCF) is one of the most prevalent electric machine failures. This study examined the stator ITSCF effects on DFIG performance for different cases. The DFIG was designed and engineered using the Finite Element Method (FEM) and the Maxwell software, and was examined in healthy operation and four defective cases with various Numbers of Inter-Turn Short Circuit Faults (NITSCF): 4, 9, 19, and 29. These models allowed the examination of the effects and the comparison of each case separately from the healthy state. The comparison was plotted in Matlab to show the effects of the faults. The novelty of this study was that it investigated the effects of different NITSCF on the performance of DFIG and not only on their effect on the stator current and distribution of magnetic flux density. A better understanding of the short circuit effects on the performance of the DFIG can be exploited for subsequent implementations of early fault detection systems.

Keywords-Doubly-Fed Induction Generators (DFIG); stator winding; Inter-Turn Short Circuit Fault (ITSCF); number of ITSCF; Finite Element Method (FEM); finite element analysis

I. INTRODUCTION

Since the 1970s, modern wind power conversion technology has been developed, especially at the end of the last century. Several Wind Turbine System (WTS) concepts were explored and different wind turbines were built [1]. Since the '90s, when the renewable energy is classified based on increasing installed capacity, wind energy occupies the first place among all types of renewable energy [2]. The ten leading countries in wind power at the end of 2017 had installed more than the three-quarters of all new wind turbines in the world [2].

DFIGs, with external [3] or inner rotors [1], are used in wind power production. As their capacity increases, their safety and reliability become more important. The variation in speed is possible due to power electronics, which are required to provide a connection to the grid. Many studies dealt with DFIG grid connection issues for different purposes [4-7]. The ITSCF of the stator or rotor windings is among the most common faults of DFIGs. The effect of ITSCF on the properties of DFIG has attracted much attention during the past decade. On the other hand, many researchers investigated how to detect and localize such faults [8-12]. However, the difference in the behavior of electrical machines between normal and fault conditions must first be understood before detection and localization can be accomplished. According to [8-17], two methods exist for analyzing the ITSCF by simulation in DFIG: the analytical and the numerical. The analytical approach is based on the multi-circuit theory [18-20], and the numerical approach is usually based on FEM [21, 22]. It's critical to understand the DFIG fault simulation models and features to investigate failure mechanisms. Several studies examined a FEM simulation model of an ITSCF stator or rotor winding in DFIG [11, 23-24].

In [12], the ITSCF in the stator winding with different NITSCF was examined, but this study was limited to the stator current behavior and only took into account two stator slots: 4 and 19. In [10], the stator ITSCF was validated both by FEM simulation and experiment, however, this study was limited to the ITSCF effect on the current and only for some turns. Other studies focused only on the effect of turn-to-turn short-circuit defects on the magnetic field [25]. Authors in [23] only focused on the rotor ITSCF effect on the magnetic flux density distribution and the rotor current.

In [26], two closely related phenomena of the current spectrum of the stator and rotor were studied: ITSCF and high

Corresponding author: Hacene Mellah

www.etasr.com

Mellah et al.: The Effect of Stator Inter-Turn Short-Circuit Fault on DFIG Performance Using FEM

resistance connections, as well as their effect on the energy injected into the network in sub and super synchronous operation, and a discussion on how to tell them apart. In [24], a quantitative study was conducted on mechanical vibration, stator currents, and stator copper loss in healthy and ITSCF cases of one-third of a stator turn of DFIG using FEM. The effect of ITSCF on stator branch currents and its expression by the Total Harmonic Distortion (THD) and the vector trajectory of Park under various ITSCF cases of stator winding was studied in [27].

The current study used FEM to model and simulate the healthy and faulty state in several cases, simulating the same DFIG but with several NITSCF of one stator phase A. A comparison between healthy and faulty stator flux linkages and current of phase A and torque were examined for constant speed.

II. DFIG GEOMETRY AND THE FEM MODEL

DFIG is widely used as a principal component in a wind turbine, as shown in Figure 1, where both the stator and the rotor are connected to the power grid. Wind power (P_w) is transformed into mechanical energy by the wind turbine, and DFIG converts this mechanical energy into electric energy [1].

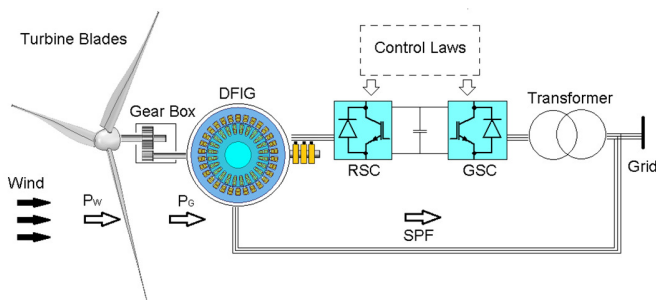


Fig. 1. Typical configuration of a DFIG WTS.

The first step in FEM is to create and draw the geometric outlines of the DFIG model based on the parameters of a selected device. Some of these parameters are listed in Table I.

TABLE I. DFIG RATED VALUES AND DESIGN PARAMETERS

Electrical and dimensional parameters	Value
Nominal output power	550 W
Nominal voltage	220 V
Given rated speed	1500 rpm
Number of pole pair	2
Number of stator slots	30
Number of rotor slots	24

The next step was to assign specific materials and their properties to each region, including copper to conductors and air to air gaps. The next step incorporated phenomena and parameters including current sources, rotor speed, boundary conditions, eddy currents, and magnetic circuit saturation. A finite element mesh was created for each DFIG part with a very fine mesh for the air gap to obtain the best results. Finally, the simulation parameters such as relative and absolute error, simulation step, and stop time were set. A 3D view of the designed DFIG is presented in Figure 2.

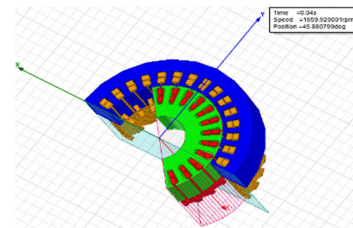


Fig. 2. 3D view of the designed DFIG.

III. SIMULATION RESULTS

This section introduces the results from the simulation of normal and faulty cases in phase A of the stator winding. Various degrees of ITSCF in the DFIG were simulated to show the effect of the NITSCF on the DFIG performance. The 2D finite element mesh of the DFIG is shown in Figure 3. Afterward, these results were used to solve the electromagnetic field equation of the DFIG. Figure 4 compares the flux linkage in the stator phase A for the normal and different numbers of ITSCF. It was observed that a greater number of short-circuit inter-turn faults increased the error between the normal and fault value, with the flux magnitude for 29 short-circuit faults being the smallest of all cases. Figures 5 and 6 demonstrate the effect of the faults in phases A, B, and C in terms of the flux. As can be observed, this effect is small but not negligible.

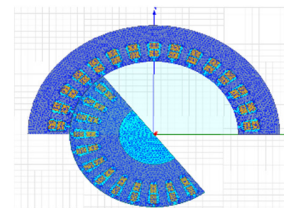


Fig. 3. 2D Finite element mesh of the DFIG

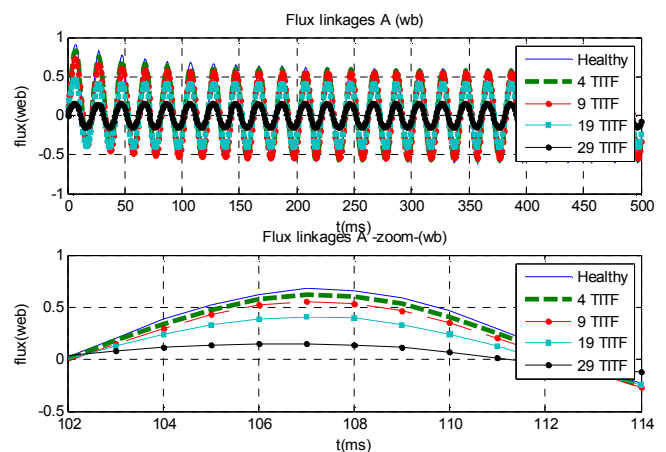


Fig. 4. Flux linkage of the stator phase A in normal and under different NITSCF conditions.

Figure 7 shows the comparison of a faulty-healthy Root Mean Square (RMS) ratio of the flux linkage of stator phases for different NITSCF. In phase A, where the different defaults are created, the flux linkage RMS value decreased for each

NITSCF increase. This decrease in flux can be explained by the decrease in the number of turns of phase A.

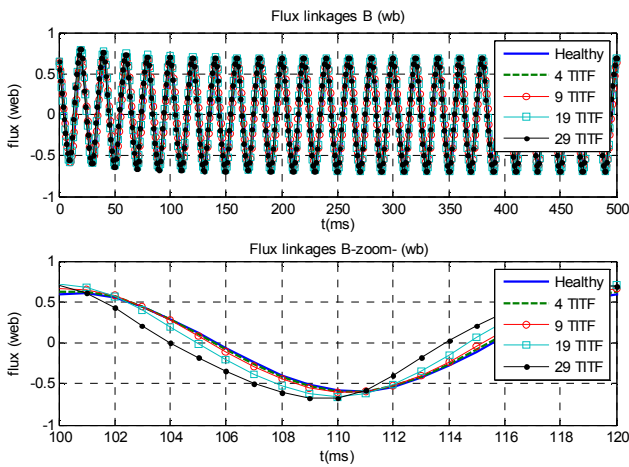


Fig. 5. Flux linkage in stator phase B for normal and various NITSCF conditions in phase A.

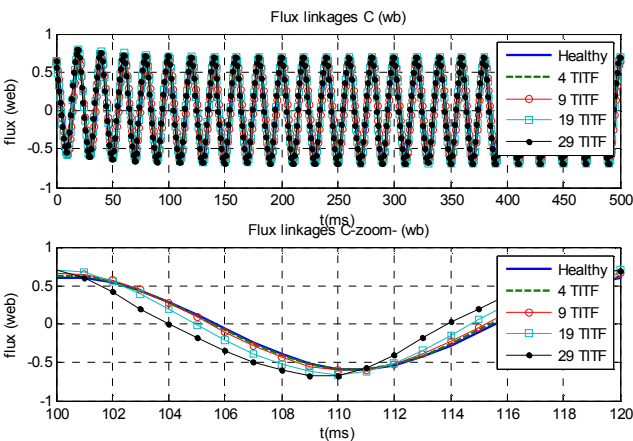


Fig. 6. Flux linkage in a stator phase C for normal and various NITSCF conditions in phase A.

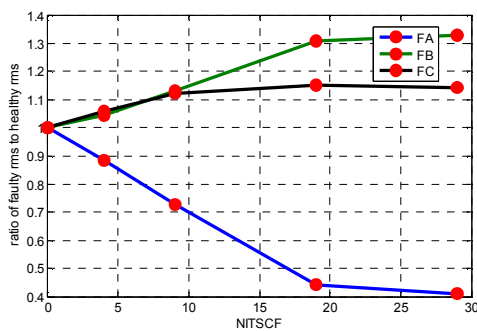


Fig. 7. Comparison of the faulty-healthy RMS ratio of stator phases for different NITSCF.

However, the opposite is noticeable for both healthy phases B and C, where the effective flux binding values increase with each NITSCF increase, especially for phase B starting from the

case of 9 NITSCF. Figure 8 shows the stator current in phase A for normal and various NITSCF in the stator winding. A short-circuit would increase the stator current and result in overheating of the winding. This can be detrimental to the machine and decrease its lifetime, and if the current exceeds the maximum short-circuit can result in its destruction. Figures 9 and 10 show the effect of NITSCF in phase A on current in phases B and C respectively. It can be observed that the effects in phases B and C are important, as the current amplitude in the condition of short-circuit results in system unbalance. Figure 11 shows a comparison of the faulty-healthy RMS ratio of the stator phases current for different NITSCF. The partial short-circuit of turns in phase A increases rapidly the current RMS value for each NITSCF rise. Moreover, at the same time, the current RMS value of the two healthy phases continues to increase with each increase in NITSCF, but in a lower order compared to the RMS value of the defective phase. Figure 12 shows the induced voltage of phase A in healthy and faulty operation. The induced voltage in phase A decreases with each NITSCF increment because the total induced voltage is a sum of the induced voltage for each turn. Figure 13 shows the induced voltage of phase B in healthy and faulty operation.

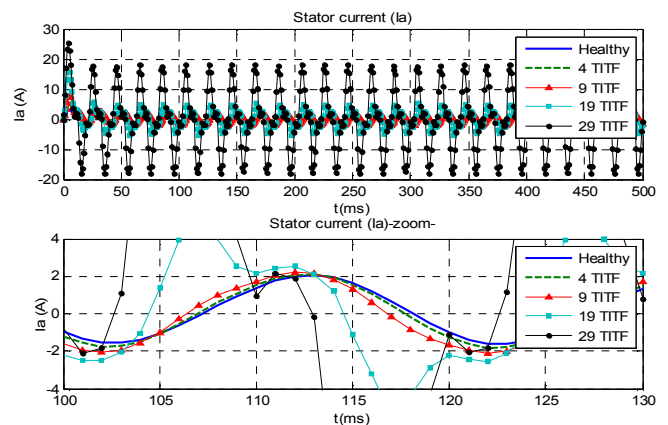


Fig. 8. Stator currents of phase A for healthy and various NITSCF conditions.

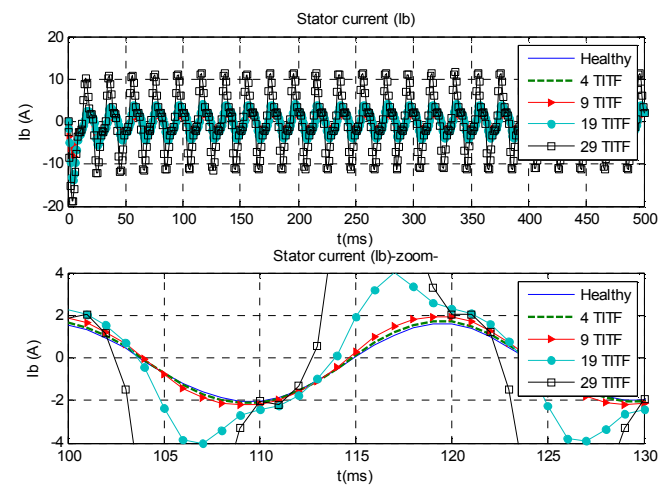


Fig. 9. Stator currents of phase B in healthy and under various NITSCF in phase A of the stator.

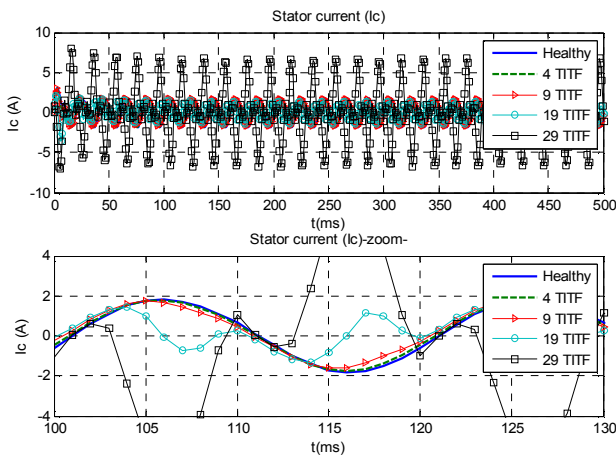


Fig. 10. Stator currents of phase C in healthy and various stator winding fault conditions of phase A.

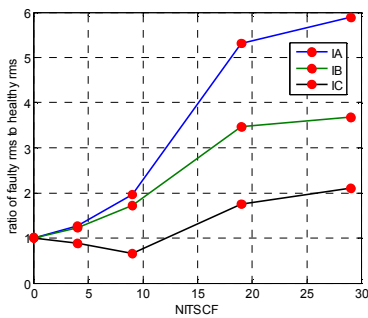


Fig. 11. Comparison of the faulty-healthy RMS ratio of the stator phase currents for various NITSCF.

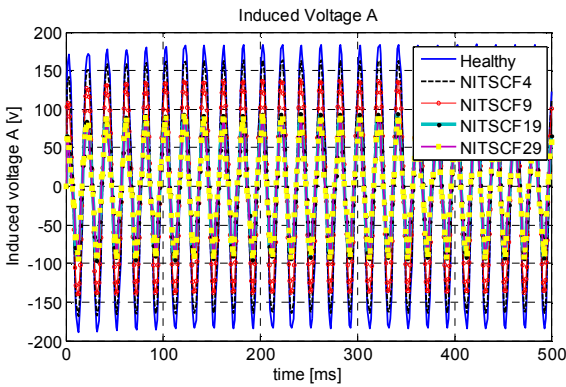


Fig. 12. Stator induced voltage of phase A in healthy and under various stator winding fault conditions.

Figure 14 displays the induced voltage of phase C in healthy and faulty operation, while Figure 15 shows the rotor currents. As can be noted, the rotor currents are not affected by the stator ITSCF. Figure 16 displays the torque curves of the DFIG at nominal load in healthy and under various NITSCF cases. This Figure summarizes the effect of inter-turn faults on DFIG torque. As can be observed, the inter-turn faults create an oscillation that increases with increasing NITSCF.

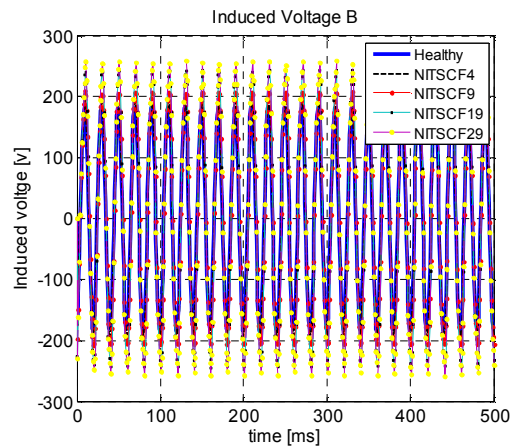


Fig. 13. Stator induced voltage of phase B in healthy and various NITSCF conditions in phase A of the stator.

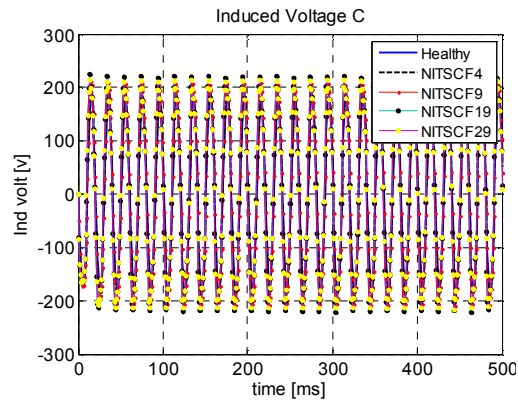


Fig. 14. Stator currents of phase C in healthy and various NITSCF in phase A of the stator.

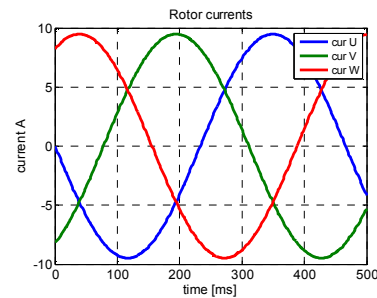


Fig. 15. Rotor currents.

Figure 17 shows the distribution of the magnetic flux density for normal and different stator winding fault conditions in phase A. As can be noted, the magnetic field is concentrated in both the stator and rotor regions and will increase both rotor and stator leakage reactance. The magnetic saturation will also increase in these regions. In the faulty state, asymmetric behavior will occur in the torque induced by the generator due to the change in currents passing through the stator winding. In this case, NITSCF increase causes an increase in torque ripple, as can be observed in Figure 17.

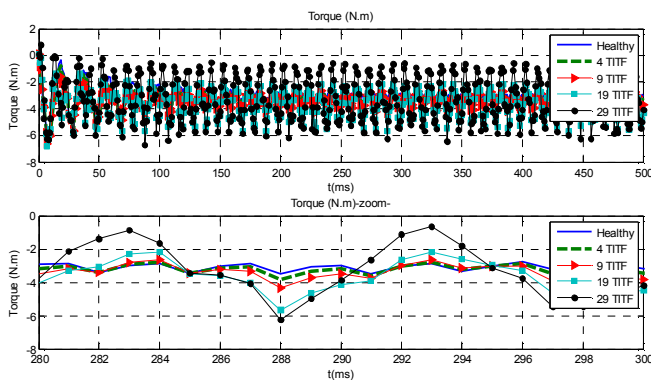


Fig. 16. Torque in healthy and various stator winding fault conditions.

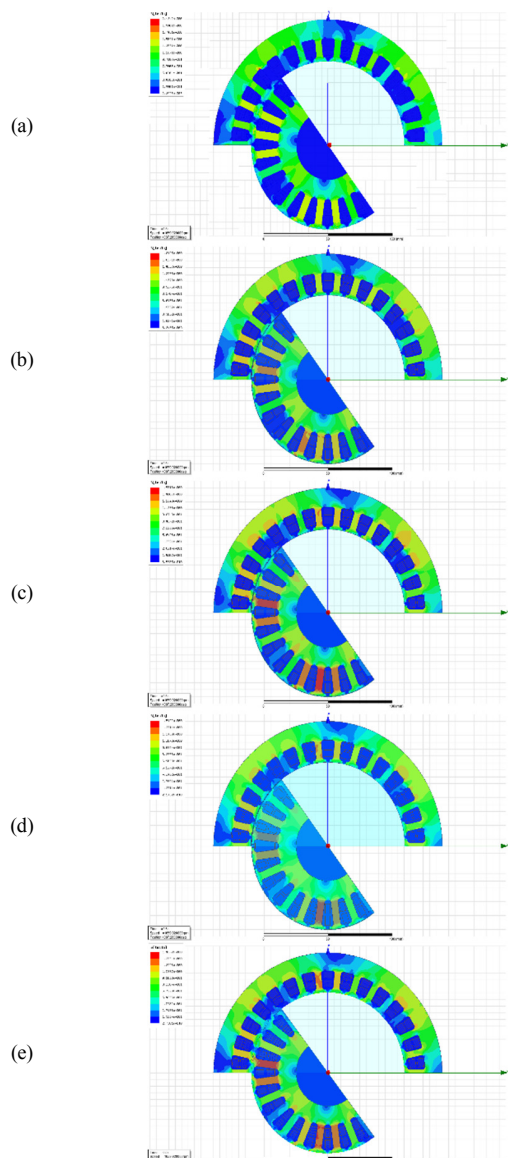


Fig. 17. The magnetic field for healthy and faulty DFIG on different cases of inter-turn short-circuited numbers: (a) 29 inter-turn faults, (b) 19 inter-turn faults, (c) 9 inter-turn faults, (d) 4 inter-turn faults, (e) healthy.

IV. CONCLUSION

FEM is a numerical method that allows the analysis of complex and non-linear systems and is frequently used for modeling and simulating electrical machines. This study used a FEM model to simulate and obtain a comparative analysis between the normal and several cases of ITSCF for one stator phase of DFIG. A comparison of stator flux, currents, induced voltage, and torque between normal and fault conditions was presented at a constant speed. ITSCF in the stator winding causes a substantial increase in branch current and a small increase in currents of B and C stator phases. ITSCF in phase A of the stator winding causes a decrease in flux in this phase and a smaller decrease in the other two phases. Moreover, ITSCF creates oscillations in the torque that increase with increasing NITSCF. An increasing number of inter-turn short-circuits causes DFIG characteristics to deviate further from normal. This study provides insight into the effects of ITSCF and can be exploited to allow the development of reliable fault detection systems and improve the quality of the electrical power injected into the power grid by WTS.

ACKNOWLEDGMENT

The authors express their gratitude and acknowledge the financial support received from the University of Setif-1 in Algeria for the PRFU Research Project under Grant A01 L07 UN1901 2019 0002.

REFERENCES

- [1] H. Mellah and K. E. Hemsas, "Design and Simulation Analysis of Outer Stator Inner Rotor Dfig by 2D and 3D Finite Element Analysis," *International Journal of Electrical Engineering and Technology*, vol. 3, no. 2, pp. 457–470, Sep. 2012.
- [2] S. Dawn, P. K. Tiwari, A. K. Goswami, A. K. Singh, and R. Panda, "Wind power: Existing status, achievements and government's initiative towards renewable power dominating India," *Energy Strategy Reviews*, vol. 23, pp. 178–199, Jan. 2019, <https://doi.org/10.1016/j.esr.2019.01.002>.
- [3] H. Mellah and K. E. Hemsas, "Design and Analysis of an External-Rotor Internal-Stator Doubly Fed Induction Generator for Small Wind Turbine Application by Fem," *International Journal of Renewable and Sustainable Energy*, vol. 2, pp. 1–11, 2013, <https://doi.org/10.11648/j.ijrse.20130201.11>.
- [4] A. Guediri and A. Guediri, "Study and Order of a Medium Power Wind Turbine Conversion Chain Connected to Medium Voltage Grid," *Engineering, Technology & Applied Science Research*, vol. 11, no. 3, pp. 7279–7282, Jun. 2021, <https://doi.org/10.48084/etasr.4169>.
- [5] H. Benbouhenni, A. Driss, and S. Lemdani, "Indirect active and reactive powers control of doubly fed induction generator fed by three-level adaptive-network-based fuzzy inference system – pulse width modulation converter with a robust method based on super twisting algorithms," *Electrical Engineering & Electromechanics*, no. 4, pp. 31–38, Jul. 2021, <https://doi.org/10.20998/2074-272X.2021.4.04>.
- [6] S. V. Bozhko, R. Blasco-Gimenez, R. Li, J. C. Clare, and G. M. Asher, "Control of Offshore DFIG-Based Wind Farm Grid With Line-Commutated HVDC Connection," *IEEE Transactions on Energy Conversion*, vol. 22, no. 1, pp. 71–78, Mar. 2007, <https://doi.org/10.1109/TEC.2006.889544>.
- [7] X. Tian, H. Tang, Y. Li, Y. Chi, and Y. Su, "Dynamic stability of weak grid connection of large-scale DFIG based on wind turbines," *The Journal of Engineering*, vol. 2017, no. 13, pp. 1092–1097, 2017, <https://doi.org/10.1049/joe.2017.0498>.
- [8] Y. Fu, Z. Ren, S. Wei, Y. Xu, and F. Li, "Using Flux Linkage Difference Vector in Early Inter-Turn Short Circuit Detection for the Windings of Offshore Wind DFIGs," *IEEE Transactions on Energy Conversion*, vol.

- 36, no. 4, pp. 3007–3015, Sep. 2021, <https://doi.org/10.1109/TEC.2021.3073007>.
- [9] O. Imoru, F. V. Nelwamondo, A. Jimoh, and T. R. Ayodele, "A neural network approach to detect winding faults in electrical machine," *International Journal of Emerging Electric Power Systems*, vol. 22, no. 1, pp. 31–41, Feb. 2021, <https://doi.org/10.1515/ijeeps-2020-0161>.
- [10] Y. Chen *et al.*, "Numerical Modeling, Electrical Characteristics Analysis and Experimental Validation of Severe Inter-Turn Short Circuit Fault Conditions on Stator Winding in DFIG of Wind Turbines," *IEEE Access*, vol. 9, pp. 13149–13158, 2021, <https://doi.org/10.1109/ACCESS.2021.3050876>.
- [11] A. U. Rehman, Y. Chen, Y. Zhao, Y. Cheng, Y. Zhao, and T. Tanaka, "Detection of Rotor Inter-turn Short Circuit Fault in Doubly-fed Induction Generator using FEM Simulation," in *2018 IEEE 2nd International Conference on Dielectrics (ICD)*, Budapest, Hungary, Jul. 2018, <https://doi.org/10.1109/ICD.2018.8514641>.
- [12] S. He, X. Shen, and Z. Jiang, "Detection and Location of Stator Winding Interturn Fault at Different Slots of DFIG," *IEEE Access*, vol. 7, pp. 89342–89353, 2019, <https://doi.org/10.1109/ACCESS.2019.2926538>.
- [13] J. Cheng, H. Ma, S. Song, and Z. Xie, "Stator Inter-turn Fault Analysis in Doubly-Fed Induction Generators using rotor current based on Finite Element Analysis," in *2018 IEEE International Conference on Progress in Informatics and Computing (PIC)*, Suzhou, China, Sep. 2018, pp. 414–419, <https://doi.org/10.1109/PIC.2018.8706293>.
- [14] H. Sabir, M. Ouassaid, and N. Ngote, "Diagnosis of Rotor Winding Inter-turn Short Circuit Fault in Wind Turbine Based on DFIG using Hybrid TSA/DWT Approach," in *2018 6th International Renewable and Sustainable Energy Conference (IRSEC)*, Rabat, Morocco, Sep. 2018, pp. 1–6, <https://doi.org/10.1109/IRSEC.2018.8703006>.
- [15] K. Ma, J. Zhu, M. Soltani, A. Hajizadeh, and Z. Chen, "Inter-Turn Short-Circuit Fault Ride-Through for DFIG Wind Turbines," *IFAC-PapersOnLine*, vol. 53, no. 2, pp. 12757–12762, Jan. 2020, <https://doi.org/10.1016/j.ifacol.2020.12.1916>.
- [16] F. Bouaziz, O. Awedni, and L. Krichen, "Modelling and fault diagnosis of rotor inter turn short circuit fault in a doubly fed induction generator-based wind turbine," in *2020 20th International Conference on Sciences and Techniques of Automatic Control and Computer Engineering (STA)*, Monastir, Tunisia, Sep. 2020, pp. 189–194, <https://doi.org/10.1109/STA50679.2020.9329344>.
- [17] S. M. M. Moosavi, J. Faiz, M. B. Abadi, and S. M. A. Cruz, "Comparison of rotor electrical fault indices owing to inter-turn short circuit and unbalanced resistance in doubly-fed induction generator," *IET Electric Power Applications*, vol. 13, no. 2, pp. 235–242, 2019, <https://doi.org/10.1049/iet-epa.2018.5528>.
- [18] D. B. Minh, L. D. Hai, T. L. Anh, and V. D. Quoc, "Electromagnetic Torque Analysis of SRM 12/8 by Rotor/Stator Pole Angle," *Engineering, Technology & Applied Science Research*, vol. 11, no. 3, pp. 7187–7190, Jun. 2021, <https://doi.org/10.48084/etasr.4168>.
- [19] Z. Xing, Y. Gao, M. Chen, and J. Xu, "Fault Diagnosis of Inter-turn Short Circuit of Permanent Magnet Synchronous Wind Turbine under the Random Wind," in *2021 IEEE 2nd China International Youth Conference on Electrical Engineering (CIYCEE)*, Sep. 2021, pp. 1–6, <https://doi.org/10.1109/CIYCEE53554.2021.9676777>.
- [20] Z. T. Mei, G. J. Li, Z. Q. Zhu, R. Clark, A. Thomas, and Z. Azar, "Scaling Effect on Inter-Turn Short-Circuit of PM Machines for Wind Power Application," in *2021 IEEE International Electric Machines Drives Conference (IEMDC)*, Hartford, CT, USA, Feb. 2021, pp. 1–8, <https://doi.org/10.1109/IEMDC47953.2021.9449606>.
- [21] M. Hussain, A. Ulasyar, H. S. Zad, A. Khattak, S. Nisar, and K. Imran, "Design and Analysis of a Dual Rotor Multiphase Brushless DC Motor for its Application in Electric Vehicles," *Engineering, Technology & Applied Science Research*, vol. 11, no. 6, pp. 7846–7852, Dec. 2021, <https://doi.org/10.48084/etasr.4345>.
- [22] Z. Tan, X. Song, W. Cao, Z. Liu, and Y. Tong, "DFIG Machine Design for Maximizing Power Output Based on Surrogate Optimization Algorithm," *IEEE Transactions on Energy Conversion*, vol. 30, no. 3, pp. 1154–1162, Sep. 2015, <https://doi.org/10.1109/TEC.2015.2411153>.
- [23] L. Jun-qing and W. Xi-mei, "FEM analysis on interturn fault of rotor winding in DFIG," in *2013 International Conference on Electrical Machines and Systems (ICEMS)*, Busan, South Korea, Jul. 2013, pp. 797–802, <https://doi.org/10.1109/ICEMS.2013.6713154>.
- [24] S. He, X. Shen, Y. Wang, and W. Zheng, "Characteristic Factor Analysis on Stator Winding Inter-turn Fault in DFIG Based on FEM Simulation," in *2017 International Conference on Computer Technology, Electronics and Communication (ICCTEC)*, Dalian, China, Sep. 2017, pp. 209–213, <https://doi.org/10.1109/ICCTEC.2017.00052>.
- [25] L. Jun-qing, M. Li, and W. De-yan, "Influence of stator turn-to-turn short-circuit on magnetic field of DFIG," in *2011 International Conference on Electrical Machines and Systems*, Beijing, China, Dec. 2011, pp. 1–5, <https://doi.org/10.1109/ICEMS.2011.6073523>.
- [26] M. Afshari, S. M. M. Moosavi, M. B. Abadi, and S. M. A. Cruz, "Study on Inter-Turn Short Circuit Fault and High Resistance Connection in the Stator of Doubly-Fed Induction Generators," in *7th Iran Wind Energy Conference (IWEC2021)*, Shahrood, Iran, Feb. 2021, pp. 1–6, <https://doi.org/10.1109/IWEC52400.2021.9467018>.
- [27] Y. Chen *et al.*, "FEM simulation and analysis on stator winding inter-turn fault in DFIG," in *2015 IEEE 11th International Conference on the Properties and Applications of Dielectric Materials (ICPADM)*, Sydney, NSW, Australia, Jul. 2015, pp. 244–247, <https://doi.org/10.1109/ICPADM.2015.7295254>.